Calculation of Transonic Flow over Supercritical Airfoil Sections

William C. Rose* and Arnan Seginer†
NASA Ames Research Center, Moffett Field, Calif.

Two numerical methods for calculating the transonic flow, including viscous effects over lifting airfoil sections and experimental data, are compared for turbulent flow over a supercritical airfoil. In addition, results for a NACA 64A010 airfoil at nonzero angle of attack are compared to demonstrate the applicability of the numerical methods to classical, lifting airfoils. One numerical method is a solution to the time-averaged Navier-Stokes equations throughout the entire flowfield. The other is a hybrid method that combines inviscid, boundary-layer, and Navier-Stokes equations in appropriate regions of the flowfield. Both methods adequately predict the surface pressures and flowfield about the 64A010 airfoil at $M=0.8$ and $\alpha=2$ deg when an appropriate turbulence model is used. The methods are not as successful for the supercritical airfoil. With the hybrid methods, the computation time can be reduced by 10:1 at little or no increase in man-hour effort required to obtain a solution. The validity of the comparison of computed results with experimental data is questionable in view of a new insight into wind-tunnel wall effects.

Nomenclature

C = chord length
C_f = skin friction coefficient, $\tau_w/\frac{1}{2}\rho_\infty U_\infty^2$
C_p = pressure coefficient, $(p-p_\infty)/\frac{1}{2}\rho_\infty U_\infty^2$
F = wind-tunnel slotted wall parameter
M = Mach number
p = static pressure
Re_c = Reynolds number based on chord, $\rho_\infty U_\infty c/\mu_\infty$
X = streamwise length
Y = airfoil section coordinate perpendicular to chord
U = streamwise velocity component
α = angle of attack
ρ = fluid density
μ = fluid viscosity

Subscripts

eff = effective
set = geometric (for angle of attack)
w = wall conditions
∞ = upstream conditions

Introduction

SEVERAL numerical methods are now available for solving the transonic flow over airfoil sections, including the turbulent boundary-layer.[1-5] The simpler, interactive methods[5] are adequate for computing weak interactions characteristic of cruise conditions, but these methods fail in strong interactions that are encountered in high-lift situations characteristic of maneuvering flight. Despite the continuing interest in calculating the flow over practical, lifting airfoil sections, the published calculations[1-4] with existing numerical codes, which can treat strong interactions, have concentrated on relatively simple airfoil sections, such as circular arc and other nonlifting symmetrical sections. Most of the published solutions from the more sophisticated Navier-Stokes codes[1,2] or the hybrid method[3] have been obtained to demonstrate the validity of the numerical procedures (commonly called "code verification") and do not present the methods as completed, off-the-shelf techniques for airfoil design. Thus, it has been appropriate in the past to examine the simplest two-dimensional airfoil configurations. Enough evidence has now been gathered to conclude that, althought quite expensive by today's standards, the sophisticated methods can describe the flow over simple configurations with the correct turbulence model. These methods must be used to calculate details of flowfields when there is extensive flow separation. This does not mean, however, that the effects of the turbulent flowfield on a parameter such as surface pressure cannot be calculated by a method that used a classical combination of inviscid and viscous effects.[5]

At present, the Navier-Stokes and hybrid (inviscid, viscous, Navier-Stokes) methods have not been applied for lifting airfoil sections, such as the supercritical sections being considered for use in fuel conservative aircraft, general aviation, and rotor aerodynamics. This paper applied the methods of Refs. 3 and 6 to transonic flow over a supercritical airfoil section designed by Yoshihara (private communication). The airfoil section geometry is described in Fig. 1 and Table 1. In addition to these methods, the results from a purely inviscid technique[7] and a classical combination of inviscid and viscous theories[5] are shown for comparison. Since the step from previous solutions of simple configurations to the lifting supercritical section is rather large, this paper also applies the various methods to a lifting symmetrical section, the NACA 64A010.

Numerical Techniques

All numerical methods used here are discussed in detail elsewhere.[3,5-7] Here these methods are applied to new configurations; therefore, the methods themselves are discussed only briefly, but modifications necessary to make them applicable to the new configurations are described.

The time-averaged Navier-Stokes equations are solved throughout the entire flowfield with the method published recently by Deiwert,[6] which includes the new MacCormack[8] speed-up algorithm. Computation time is reduced significantly with this new algorithm. The method can compute the flow over two-dimensional lifting airfoils of arbitrary section. The flowfield above, below, and upstream of the airfoil and the wake are computed without an assumption of symmetry. This method is potentially powerful in that only the airfoil geometry must be input once a computational mesh and turbulence model are established.

Presented as Paper 77-681 at the AIAA 10th Fluid and Plasmadynamics Conference, Alburquerque, N. Mex., June 27-29, 1977; submitted July 22, 1977; revision received April 3, 1978.

Index categories: Computational Methods; Transonic Flow.
*Research Scientist. Member AIAA.
†National Research Council Senior Research Associate. Member AIAA.

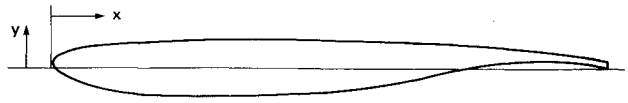

Fig. 1 Supercritical airfoil geometry used in the present study (Yoshihara, private communication).

The hybrid method[3] uses an iteractive procedure to combine solutions of the inviscid small-perturbation transonic equation,[7] boundary-layer equation,[9] and Navier-Stokes equations[10] in appropriate regions of the flowfield. Here this method is used exactly as described in Ref. 3. It was, however, necessary to modify the inviscid code to allow computation when a large radius bluntness of the leading edge is present, such as on the supercritical airfoil section. Conceptually, any inviscid method can be used by this technique; however, the method in Ref. 7 is highly desirable since it allows for modeling wind-tunnel wall effects.

A classical combination of inviscid and viscous solutions[5] is used here without modification. The method solves the full potential equation in a transformed plane that maps the airfoil into a circle. Viscous effects are modeled by a simple ad hoc procedure that computes the displacement thickness of the attached boundary-layer and assumes an effective boundary, representing the displacement effect once separation has occurred.

Finally, results from the inviscid, small-disturbance method of Murman et al.[7] are shown for a nonconservative shock-capturing difference algorithm. Although strictly inconsistent with inviscid concepts, the nonconservative formulation seems to agree better with experimental data than the fully conservative algorithm. Thus, it is used extensively. Of course, no amount of precise numerical computation will show the correct behavior of strongly interacting turbulent flows without a physically realistic model of the turbulent Reynolds stresses. Although numerous models of the turbulent mixing in boundary layers similar to those present on transonic airfoils have been proposed. The ones of practical consideration are still those based on algebraic expressions that relate turbulent Reynolds stresses to mean flow. Because of the enormous increases in computer time required for any but the simplest turbulence model, more sophisticated models are not currently considered as engineering tools, despite the fact that they might better represent the fluid physics. The first model used here is the simple Cebeci-Smith model denoted "baseline"[11] at Ames Research Center. Since it is generally recognized that such models are inadequate to describe strongly interacting flows, attempts were made to modify so-called equilibrium algebraic turbulence models to account for nonequilibrium effects in transonic airfoil calculations.[2] Based on the results presented in Ref. 2 which indicated a need to reduce the turbulent mixing in the separated flow, we proposed[12] a limiting form of that class of models which essentially eliminates turbulent mixing in the separated flow. This model seems to give a better numerical description of the flow over transonic airfoils when separation is present but it has not been verified experimentally. This model, denoted as the "S-R" model, is used here extensively.

Table 1 Upper and lower y/c values for supercritical airfoil geometry

x/c	Upper y/c	Lower y/c
.000000	.00910	.00910
.002500	.01503	.00339
.007500	.02553	-.00673
.012500	.02880	-.01020
.017500	.03043	-.01260
.022500	.03203	-.01528
.027500	.03331	-.01763
.032500	.03423	-.01945
.037500	.03500	-.02100
.045000	.03617	-0.2316
.055000	.03759	-.02581
.065000	.03866	-.02815
.075000	.03953	-.03026
.085000	.04033	-.03221
.097500	.04123	-.03453
.115000	.04226	-.03775
.140625	.04367	-.04177
.171875	.04498	-.04546
.203125	.04629	-.04782
.234375	.04738	-.04900
.265625	.04841	-.04947
.296875	.04907	-.04992
.328125	.04953	-.05004
.359375	.04984	-.04988
.390625	.05001	-.04949
.421875	.05009	-.04875
.453125	.05003	-.04764
.484375	.04978	-.04620
.515625	.04933	-.04429
.546875	.04874	-.04177
.578125	.04805	-.03847
.609375	.04708	-.03401
.640625	.04585	-.02790
.671875	.04462	-.02050
.703125	.04295	-.01327
.734375	.04115	-.00740
.765625	.03935	-.00283
.796875	.03746	.00111
.828125	.03541	.00429
.859375	.03319	.00683
.885000	.03115	.00810
.900000	.02973	.00853
.915000	.02815	.00857
.930000	.02651	.00825
.945000	.02481	.00753
.960000	.02287	.00654
.975000	.02040	.00446
.990000	.01722	.00184
1.000000	.01500	0.00000

Experimental Data

Experimental data for two two-dimensional airfoil sections are considered here. Both sections of 15-cm chord were tested at $Re_c = 2 \times 10^6$. The data for the NACA 64A010 are from two studies – one published[13] and the other conducted recently by D.A. Johnson and W.D. Bachalo. The data considered here are surface-pressure distributions and density contour obtained from an infinite-fringe interferometric reconstruction of a hologram for $M = 0.8$, and an effective free-air angle of attack of 2 deg. The data from Ref. 13 are interpolated to give an effective angle of 2 deg. The Johnson-Bachalo data were obtained at $\alpha_{set} = 3.5$ deg in the wind tunnel, producing an effective 2 deg angle of attack. The effective angles in both cases were determined from tunnel corrections based on previous tests (Stivers, private communication) of the 64A010 airfoil section at similar conditions in the same wind tunnel.

The data for the supercritical airfoil section considered here were obtained during the present investigation by the present authors and S.V. Murthy. These data consist of surface-pressure distributions and quantitative skin friction measurements[14] at $M = 0.8$ and a set angle of attack of 2.0 deg. The corrected effective free-air angle of attack for this case was 0.24 deg. However, during our study it became evident that this correction was wrong and that the effective angle for this case was approximately 1 deg.

An important feature of the present experimental data is that they were obtained in the Ames 2-ft × 2-ft wind tunnel, which has slotted upper and lower surfaces, corresponding to the suction and pressure surface of the airfoil. These slotted walls allow an unknown mass and momentum flux to exit and return to the flow along the entire tunnel test section. The slotted walls do not, by any means, produce an equivalent free-air flow at the same angle of attack. Therefore, in using the data for numerical code verification, one must constantly be aware that the boundary conditions in the wind-tunnel case are neither solid-wall nor free-air conditions. The common practice is to assume that free-air conditions prevail at the corrected angle of attack. However, this assumption is unsubstantiated.

Of course, much more data than used here were obtained for the two airfoil sections. However, the data presented for

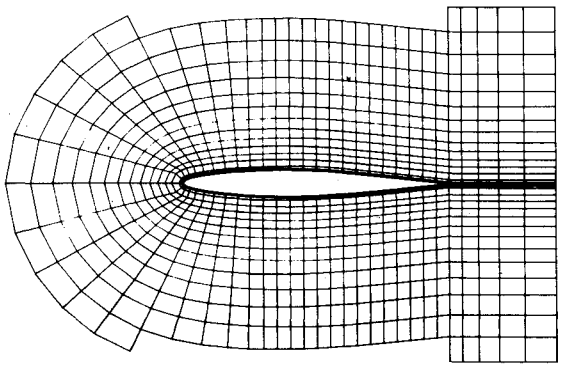

Fig. 2 Computational mesh used for the NACA 64A010 airfoil in the method of Ref. 6.

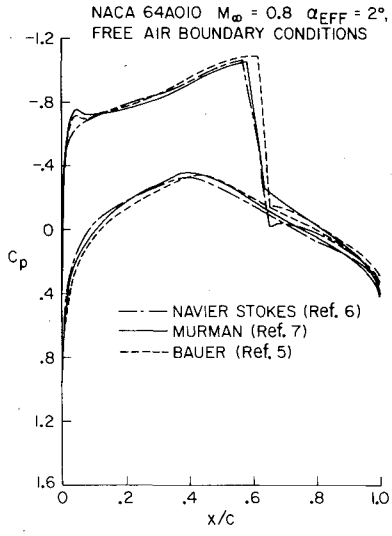

Fig. 3 Comparison of solutions from the Navier-Stokes method[6] using slip conditions with inviscid solutions.

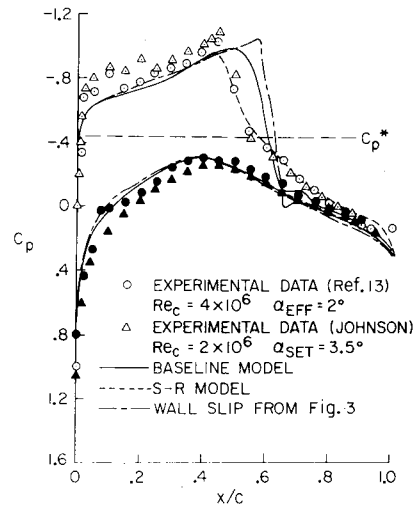

Fig. 4 Comparison of Navier-Stokes solutions with experimental data; pressure distribution over a NACA 64A010 airfoil: $M = 0.8$, $Re_c = 2\times10^6$, $\alpha_{eff} = 2.0$ deg.

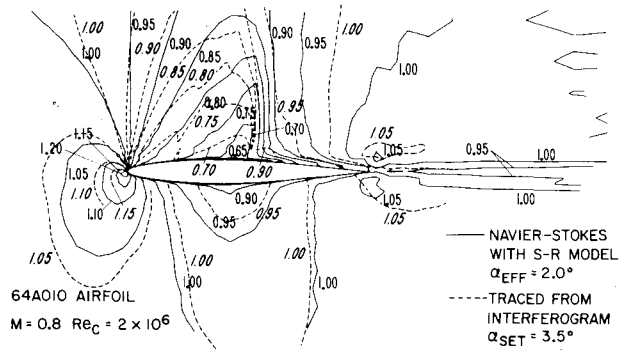

Fig. 5 Comparison of calculated and experimental density contours: 64A010 airfoil, $M = 0.8$, $Re_c = 2\times10^6$

comparison are representative of practical situations for lifting airfoils. The data are discussed further when compared with the various numerical methods.

Results and Discussion

The results of the numerical methods are now compared with themselves and with experimental data. The numerical methods and data are further discussed where appropriate. The comparisons for the NACA 64A010 airfoil are presented first to establish the applicability of the methods to a lifting but symmetrical section. The results of the full Navier-Stokes method are discussed first, then the results of the hybrid method. Results of other methods are also considered here for comparison.

In any numerical technique involving the discretization of the differential equations of fluid motion, a mesh or computational grid must be chosen. In inviscid methods, a dense grid is generally used without a second thought since the resulting computation time is so small. However, this is not the case when one establishes a mesh for the much costlier Navier-Stokes codes. As previously shown,[15] in order to have any confidence in a Navier-Stokes solution including viscous effects, one must insure that the chosen mesh can correctly represent the essentially inviscid portion of the flowfield. This was done for the mesh shown in Fig. 2, which produced the calculated surface-pressure distribution shown in Fig. 3. Along with the Navier-Stokes solution, the solutions from Refs. 5 and 7 are shown. Agreement among the various calculations gives confidence in the difference algorithm and mesh used for the Navier-Stokes code. The casual reader should not, however, be lulled into thinking that this is a trivial comparison, because it is not at all difficult to choose numerous meshes that simply will not resolve the basic features of the flow. Both results from the methods of Refs. 5 and 7 are for nonconservative difference formulations of the shock wave; hence, there is a numerical viscosity in the shock region. Both methods are thus not purely inviscid, although a wall slip condition of inviscid flow was imposed. The Navier-Stokes "inviscid" result was also obtained by use of a wall slip condition, but with the actual molecular viscosity. The Navier-Stokes solution clearly does not have the detailed resolution near the leading edge that the other inviscid solutions have. Since the inviscid solutions have at least three times more grid points in this region, the cost for duplicating this grid density in the Navier-Stokes code could be beyond practical limits. Note that, despite the lack of detail near the leading edge, the Navier-Stokes solution does predict essentially all of the downstream region within engineering accuracy. When a usable mesh was established, the viscous no-slip condition was imposed at the airfoil surface and the turbulent shear stress model was activated.

Results for two turbulence models used in the Navier-Stokes method are compared (Fig. 4) with the experimental surface-pressure data for a 2 deg effective angle of attack. Also included for comparison is the inviscid surface-pressure curve from Fig. 3. As shown, there is only a slight change in the pressure distribution from the inviscid curve to the one computed using the baseline model. To produce any substantial change in the pressure distribution and in the location of the computed shock wave, the S-R turbulence model[12] had

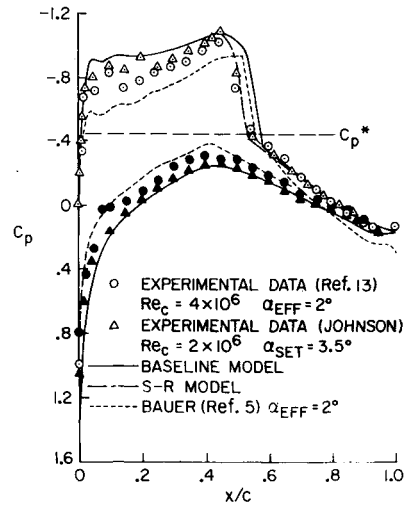

Fig. 6 Comparison of hybrid method results with experimental data; pressure distribution over a NACA 64A010 airfoil: $M = 0.8$, $Re_c = 2\times10^6$, $\alpha_{set} = 3.5$ deg.

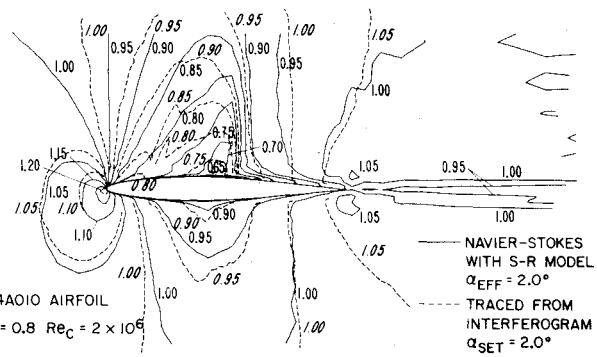

Fig. 7 Comparison of calculated and experimental density contours: NACA 64A010 airfoil, $M = 0.8$, $Re_c = 2\times10^6$.

to be used. Since the interaction between the shock wave and the turbulent boundary layer is very strong in the present case, the S-R model would appear to be required[12] and, in fact, does produce a calculation in essential agreement with experimental data.

Since it has been well established that surface pressures are the least sensitive to the computational techniques and flowfield model, we compared the full flowfield solution with the experimental data. Such a comparison and an indication of the quantitative agreement of calculations and experiment are shown in Fig. 5. The experimental data are density contours from an infinite fringe interferogram. There is a general agreement between the Navier-Stokes code using the S-R model and the data. The exception is in the upstream region where the density contours differ and the experimental pressures are slightly lower (Fig. 4). Since the results in Fig. 3 indicate that the present mesh cannot resolve the expansion around the immediate leading-edge region, one might question the validity of the calculations. However, Fig. 3 also indicates that, once the leading-edge region is passed, the Navier-Stokes code agrees with an inviscid solution known to be accurate. Thus, it is likely that either the free-air solution does not represent the wind-tunnel flow conditions or the stated angle of attack is incorrect. Since the angle of attack is deduced and is not a primitive measurement, it is probably the most likely source of uncertainty. Unfortunately, the effect of not knowing the angle of attack for code verification purposes is one of first order and might cloud any real comparison.

To resolve the question of wind-tunnel wall effects, the hybrid method,[3] which includes a slotted wall calculation

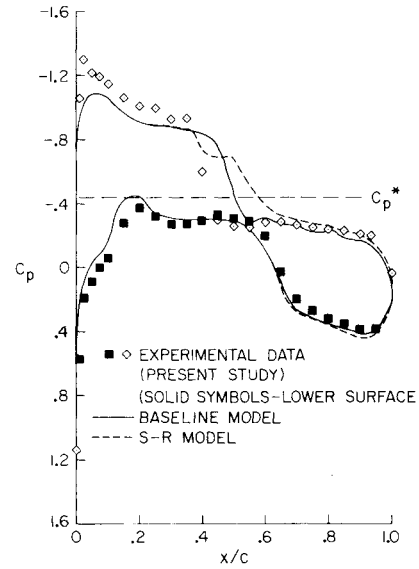

Fig. 8 Comparison of Navier-Stokes solutions with experimental data; pressure distribution, supercritical airfoil: $M = 0.8$, $Re_c = 2\times10^6$, $\alpha_{eff} = 1.0$ deg.

capability, was next applied to the 64A010 section. A wall slot parameter of $F = 0.03876$, appropriate for this wind tunnel, was used. Figure 6 compares the results from the hybrid method with the same experimental data discussed in Fig. 4. The pressure distribution calculated by the hybrid method generally agrees well with experimental data, especially when the S-R turbulence model is used. The agreement on the aft section of the airfoil is very good, while on the front section the calculated pressures are slightly low on the suction surface and slightly high on the pressure surface. This variance may be attributed to the error introduced by the small perturbation assumptions. Even though the hybrid method does not suffer from insufficient resolution on the leading edge as the Navier-Stokes method did, the afore-mentioned discrepancy precludes a significant conclusion about a possible wind-tunnel effect on the flowfield. In future applications of the hybrid method, the solution of the full potential equation[5] must be used to eliminate the small-disturbance assumptions. This method, however, has not yet been modified for wind-tunnel wall boundary conditions. Another indication of a previously unknown wind-tunnel effect is shown in Fig. 7. The computed density contours at $\alpha = 2$ deg are compared with the experimental contours at $\alpha_{set} = 2$ deg. As expected, the shock positions and most of the flowfield contours disagree. However, the density contours near the leading edge are in surprising agreement. These results seem to indicate that the fore section of the airfoil sees the oncoming flow at roughly the geometric set angle of attack, while the aft section of the flowfield resembles the flow at the effective angle of attack. This phenomenon is currently being investigated.

For the 64A010 airfoil, it appears that both the full Navier-Stokes code and the hybrid method yield essentially the same surface-pressure distributions when the same turbulence model is used. Both methods adequately predict the experimental data when the S-R model is used. The classical inviscid-viscous method,[5] using an ad hoc model of the turbulent flow effects, also seems to predict the data (Fig. 6), but not successfully. Wind-tunnel wall effects cloud the comparisons somewhat. However, for this case they do not dominate the flow so much as to invalidate the preceding comparisons. No such definite conclusions can be drawn about the full flowfield solution.

With the background obtained on the 64A010, the study attempted to calculate the supercritical airfoil section. The experimental surface-pressure distribution for the super-

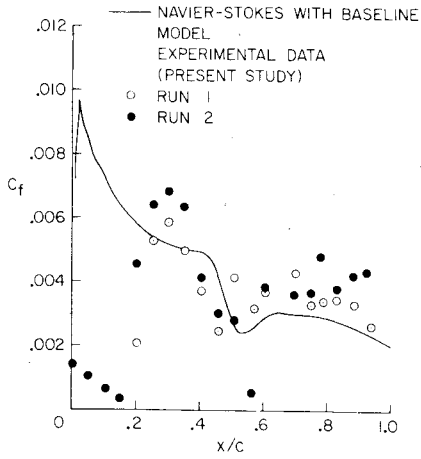

Fig. 9 Comparison of calculated and experimental skin-friction coefficients for supercritical airfoil: $M=0.8$, $Re_c=2\times10^6$, $\alpha_{eff}=1.0$ deg.

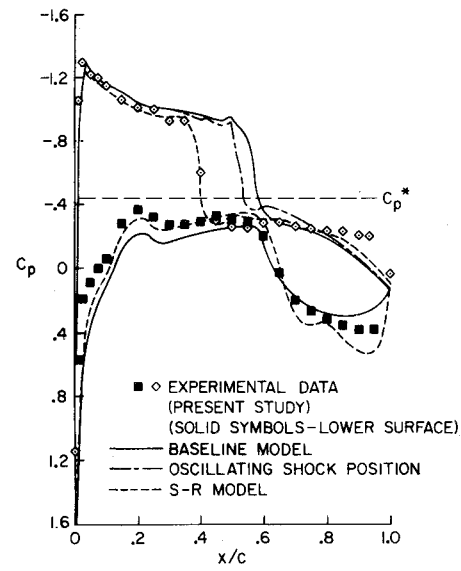

Fig. 10 Comparison of pressure distribution from the hybrid method with experimental data for supercritical airfoil: $M=0.8$, $Re_c=2\times10^6$, $\alpha_{set}=2.0$ deg.

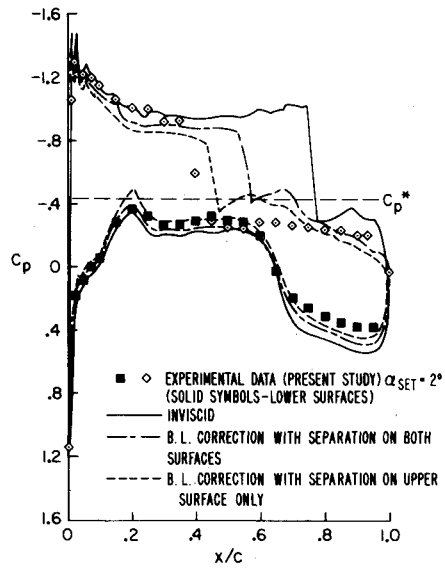

Fig. 11 Comparison of pressure distribution from the inviscid-viscous method[5] with experimental data for supercritical airfoil: $M=0.8$, $Re_c=2\times10^6$, $\alpha_{eff}=1.0$ deg.

critical airfoil section tested is shown in Fig. 8. The set angle of attack was 2 deg. Calculations from the Navier-Stokes code with the previously discussed two turbulence models are also shown in Fig. 8 for $\alpha=1$ deg. The corrected effective angle of attack according to Stivers (private communication) was 0.24 deg. However, the discrepancy between the computed results at this angle and the experimental data was so large that subsequent computations were made for an angle of 1 deg deduced (from the inviscid results with the code of Ref. 5) to be near the effective angle. Actually the effective angle is even larger, possibly 1.5 deg, as indicated by the final viscous results of this study.

The general trends of the calculations agree with experimental data, including the pressure on the concave portion of the aft lower surface. In addition, the upper-surface pressure, downstream of the shock, is well predicted by the baseline model. However, the S-R model fails to properly describe this part of the pressure distribution. A primary calculated parameter, the shock-wave strength, is not physically represented by the S-R model. This probably results because this model appears to adequately predict strong interactions, but not weak ones. The shock strength in the present case is relatively weak since the test Mach number is only slightly above that for drag divergence.

In support of the evidence that the shock interaction is relatively weak, the experimental skin-friction data (Fig. 9) indicate an attached flow over the entire upper surface. Also shown are the calculated values of C_f from the Navier-Stokes code with the baseline model. In the calculation, turbulent flow is assumed to begin at the leading edge, while, experimentally, a trip located at $x/c=0.17$ was used to induce turbulent flow. Aside from the effects of the trip, the agreement between the calculation and the data is surprisingly good.

For the surface-pressure comparisons, the results of the hybrid method are shown in Fig. 10; the inviscid-viscous method results are shown in Fig. 11. The hybrid method results with the baseline eddy viscosity model predict the shock wave at about 17% chord too far downstream. The upper-surface pressures, upstream of the shock and immediately following it, agree well with experimental data. Agreement of the rest of the pressure distribution is not as good. The pressure recovery on the trailing edge is too strong, as in Fig. 11. Most of the pressures on the lower surface are too high, while the pressures in the trailing-edge concavity are too low. Another interesting feature in the results of the hybrid computation with the baseline model (Fig. 10) is the oscillation of the shock wave between two locations. This phenomenon has not been observed in the present Navier-Stokes computation, but similar phenomena were previously observed in calculations over different airfoils[16] and also experimentally.[4] When the S-R model is used in the hybrid method, the shock is predicted quite accurately, contrary to the Navier-Stokes method where the S-R model was inadequate. The agreement between the remaining pressures and experimental data also improves. However, with this model flow separation is predicted over the aft upper surface from the shock out into the wake. Such a separation has not been observed either in the experiment or in the Navier-Stokes solution. The high pressures on the fore section of the lower surface apparently result from the inadequacy of the small-perturbation equation.

It appears that some aspects of the supercritical airfoil are easier to predict by the Navier-Stokes method that for the 64A010 section. On the other hand, the hybrid method deals more easily with the 64A010 airfoil. Again, wind-tunnel wall effects and the determination of an effective angle of attack are first-order factors that cloud the assessment of how valid the various calculation procedures are.

Table 2 CPU times on a CDC 7600

	NACA 64A010, min	Supercritical, min
Inviscid	<1	<1
Inviscid-viscous	<1	<1
Hybrid	20	40
Navier-Stokes	85	90

Computation Times and Man-Hours

The total cost of obtaining a solution to a practical engineering design problem is always of interest. What we have studied here, of course, are very simple, two-dimensional configurations that are only components of real aerodynamic devices. The costs associated with even simple configurations fall into three main categories: 1) the man-hour cost of preparing input, running codes, and presenting results; 2) the machine central processing unit (CPU) dollar cost for the final solution itself; and 3) the total dollar cost of all CPU time used in unsuccessful or inadequate computer runs used to obtain a final solution.

The man-hour costs can be easily arranged in increasing order as follows: simple inviscid methods,[7] classical inviscid-viscous methods,[5] full Navier-Stokes codes,[6] and hybrid methods.[3] This sequence assumes (the rather unlikely situation) that the first attempt to obtain a solution from any given method will be successful. The man-hour effort for the hybrid method as used here is large because, after each iteration, the convergence of the method is checked and the computation restarted. Conceptually, this could be automated, more than has been done, to reduce man effort to the level of the first three techniques. There are two major problems with this simple ordering of man-hour expenditure. First, the newer methods take more "massaging" to get a solution; second, if the desired aerodynamic configuration is one for which the operator has not had previous experience, there will be inevitable pitfalls that will extend the time needed to solve the problem.

The actual CPU times for the solutions presented here, in minutes of execution time on a CDC 7600, are shown in Table 2.

In comparing the CPU times for the hybrid and Navier-Stokes methods, note that while the Navier-Stokes code used the MacCormack speed-up algorithm, the hybrid method still uses the older and slower one. When the new algorithm is incorporated into this method, CPU times should be reduced by 75%. These times are the easiest to estimate accurately. Probably the hardest to estimate and least talked about machine times are those spent before the final acceptable solutions are obtained. It has been our experience that from 4 to 10 times more machine time is used to obtain the final solution.

The hybrid method gives a detailed resolution and physically realistic representation of the flowfield at reasonable cost. In addition, since much of the intermediate output after a single iteration costs very little, errors may be detected early and much machine time saved. This is only partially true for the full Navier-Stokes methods because it may take substantial machine time before one can detect a problem.

Concluding Remarks

Four numerical methods for calculating the transonic flow over two-dimensional airfoil sections were applied to a lifting case of NACA 64A010 airfoil section and a supercritical section. Results from the calculations were compared with surface-pressure data, flowfield density contours, and quantitative skin-friction data. Detailed agreement with the experimental data and calculations is obtained when the effects of the turbulent flow are correctly modeled. There appear to be no numerical problems associated with any of the methods for either airfoil section. The limiting factor in all the methods remains the turbulence model (or when to use a given model). Wind-tunnel wall effects included in the experimental data, but not modeled in the numerical methods, make conclusive validation of the codes impossible at this time. The full Navier-Stokes codes are expensive; the hybrid method could give about the same numerical and physical accuracy at considerably less cost.

References

[1] Deiwert, G.S., McDevitt, J.B., and Levy, L.L. Jr., "Simulation of Turbulent Transonic Separated Flow Over an Airfoil," NASA SP-347, 1975, pp. 419-436.

[2] Deiwert, G.S., "Computations of Separated Transonic Turbulent Flows," *AIAA Journal*, Vol. 14, June 1976, pp. 735-740.

[3] Seginer, A. and Rose, W.C., "A Numerical Solution of the Flow Field Over a Transonic Airfoil Including Strong Shock Induced Flow Separation," AIAA Paper 76-330, San Diego, Calif., July 14-16, 1976.

[4] McDevitt, J.B., Levy, L.L. Jr., and Deiwert, G.S., "Transonic Flow About a Thick Circular-Arc Airfoil," *AIAA Journal*, Vol. 14, May 1976, pp. 606-613.

[5] Bauer, F., Garabedian, P., Korn, D., and Jameson, A., "Supercritical Wing Sections, II. A Handbook," *Lecture Notes in Economics and Mathematical Systems*, Vol. 108, Springer-Verlag, New York, 1975.

[6] Deiwert, G.S., "Recent Computation of Viscous Effects in Transonic Flow," presented at the 5th International Conference on Numerical Methods in Fluid Dynamics. The Netherlands, June 28-July 2, 1976.

[7] Murman, E.M., Bailey, F.R., and Johnson, M.L., "TSFOIL - a Computer Code for Two-Dimensional Transonic Calculations, Including Wind-Tunnel Wall Effects and Wave-Drag Evaluations," NASA SP-347, 1975, pp. 769-778.

[8] MacCormack, R.W.,"An Efficient Numerical Method for Solving the Time-Dependent Compressible Navier-Stokes Equations at High Reynolds Number," NASA TM C-73,129, July 1976.

[9] Murphy, J.D. and Davies, C.B., "Users Guide—Ames Inlet Boundary-Layer MK-I," NASA TM X-62,211, 1973.

[10] Baldwin, B.S. and MacCormack, R.W., "Numerical Solution of the Interaction of a Strong Shock Wave with a Hypersonic Turbulent Boundary Layer," AIAA Paper 74-558, Palo Alto, Calif., 1974.

[11] Baldwin, B.S. and Rose, W.C., "Calculation of Shock-Separated Turbulent Boundary Layers," NASA SP-347, 1975, pp. 401-417.

[12] Seginer, A. and Rose, W.C., "An Approximate Calculation of the Strong Interaction on a Transonic Airfoil," AIAA Paper 77-210, Los Angeles, 1977.

[13] Steinle, F.W. Jr. and Gross, A.R., "Pressure Data from a 64A010 Airfoil at Transonic Speeds in Heavy Gas Media of Ratio of Specific Heats from 167 to 112," NASA TM X-62,468, 1975.

[14] Murthy, S.V. and Rose, W.C., "Direct Measurement of Wall Shear Stress by Buried Wire Gages in a Shock Wave Boundary-Layer Interaction Region," AIAA Paper 77-691, Albuquerque, N. Mex., 1977.

[15] Rose, W.C., "Practical Aspects of Using Navier-Stokes Codes for Predicting Separated Flows," AIAA Paper 76-96, Washington, D.C., 1976.

[16] Walitt, L., King, L.S., and Liu, C.Y., "Computation of Viscous Transonic Flow About a Lifting Airfoil," AIAA Paper 77-679, Albuquerque, N. Mex., 1977.